MOSA Monitoring Based on Analysis of the Total Leakage Current by SOM Networks

George R. S. Lira and Edson G. Costa

***Abstract*-- The majority of the metal-oxide surge arrester (MOSA) monitoring techniques are based on total leakage current (TLC) decomposition on their capacitive and resistive components. However, these techniques are subject to some financial, technical and practical limitations which can to difficult their employment on field. In this paper, a new monitoring technique for MOSA is proposed. The technique is based on feature extraction of measured TLC signals and on analysis of these characteristics by special kind artificial neural networks (ANN) called Self-Organizing Maps (SOM). The evaluated measured TLC were obtained from station class MOSA submitted to their MCOV. On the lab tests, six different kind of failures were simulated on the tested MOSA with the purpose of to evaluate the technique capacity of distinguish different operating conditions of MOSA. Hit ratios greater than 98% were obtained on identification of the operating conditions. The results show the viability of the technique on MOSA monitoring procedures.**

***Keywords*: Metal-oxide surge arresters, total leakage current, monitoring, diagnosis, artificial neural networks, parametric identification.**

I. Introduction

METAL-OXIDE surge arresters (MOSA) are equipments used for protection of electrical power systems against overvoltages. Thus, they contribute decisively for the increase on the reliability, economy and continuity of power system operation. Due to the importance of the MOSA, it is necessary the development and improvement of techniques and procedures to monitor and diagnose the MOSA operation condition correctly and accurately. Since, the surge arrester failure conduct non programmed power supply interruption, damage to other substation equipment, and risks to technical personnel.

A set of methodologies commonly applied on MOSA monitoring and diagnosis is based on the measurement and decomposition of the total leakage current (TLC) across the surge arrester on the steady state operation. The leakage current is usually decomposed in its capacitive and resistive components, since the resistive component and its third harmonic present significant variations on the magnitude and waveshape proportional to the MOSA degradation level [1]-[4]. The analysis and interpretation of these variations are the base of the most common monitoring techniques found on literature.

The main problem of the methods based on TLC decomposition is the necessity of measure the applied voltage on the surge arrester or estimate angle phase difference between the leakage current and the applied voltage. To measure the applied voltage on site is hard task, since often there are: some difficult to access and to connect data acquisition systems to measurement devices (such as potential transformers); the influence of the neighbors transmission lines on the measurement; and the influence of the parasite capacitances on the voltage phase angle along the arrester housing [4]. These troubles can to make impossible the MOSA diagnosis. There are some methods [2] that claim to overcome the difficulties mentioned, yet make use of a series of simplifications and approximations that compromise the accuracy of the results provided.

Thus, it is evident the necessity of to develop MOSA monitoring and diagnosis methods that can be applied on site more easily, showing reliable results which aid the technical substation personnel in predictive and preventive maintenance activities. In this paper, it is proposed a new technique for MOSA monitoring and diagnosis. The technique is based on analysis of the feature extracted of surge arresters total leakage current. The voltage measurement is not necessary.

II. Proposed Technique

The harmonic distortion level and the total current magnitude (especially, its resistive component) are important indicators of the MOSA degradation level [3], [4]. Thus, it seems reasonable to extract features of the total current in order to train a classifier of defects or failures. However, it is noteworthy that the approach proposed here differs from those commonly used in the literature, i.e., approaches based on decomposition of the capacitive and resistive components of the leakage current. In this paper, it is proposed that the characteristics used by the system for monitoring and diagnosis are extracted from the signal of total leakage current and not the resistive component. Thus, it avoids a number of practical and technical restrictions.

In Fig. 1 is presented an overview of the proposed methodology [5]. Initially, arresters total leakage current signal are obtained in laboratory or field. Then the signals feature extraction (relevant harmonic components) is carried out. From the extracted features is built a database of features,

G. R. S. Lira and E. G. Costa are with the Department of Electrical Engineering, Federal University of Campina Grande, Av. Aprigio Veloso, 882, Universitario, 58.429-140, Campina Grande - PB - Brazil (e-mails: george, edson@dee.ufcg.edu.br.)

Paper submitted to the International Conference on Power Systems Transients (IPST2013) in Vancouver, Canada July 18-20, 2013.

which is used in the training and testing phases of a system of classification of defects based on Artificial Neural Networks.

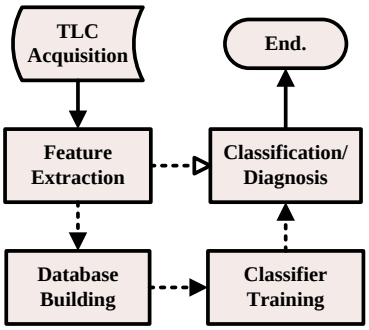

Fig. 1. Proposed methodology overview.

III. Total Leakage Current Measurements

The total leakage current was obtained from maximum continuous operation voltage (MCOV) tests carried out in laboratory for station class surge arresters. The diagram of the experimental arrangement used on the tests is shown in Fig. 2.

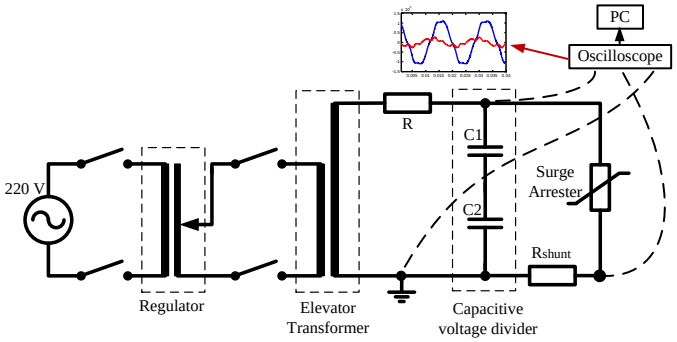

Fig. 2. Experimental arrangement diagram.

The experimental arrangement is composed by a adjustable voltage source, a voltage regulator, a elevator transformer, a protective resistance, a capacitive voltage divider, the test object (the surge arresters) in series with a *shunt* resistance. The voltage divider was used only to monitor the applied voltage. The current signal was obtained from *shunt* resistance and a data acquisition system composed by voltage probes, digital oscilloscope, and a PC.

A. Evaluated Samples

The testing of MCOV application and current measurement was carried out in some station class surges arrester with rated voltage and MCOV of 92 kV and 76 kV, respectively. These equipments had different levels of conservation. The evaluated surge arresters had their levels and types of degradation changed during the tests, by inserting failures produced artificially in laboratory. Altogether, 07 different types of MOSA operating conditions were evaluated in the tested samples. The conditions corresponded to the good condition and typical failures found in surge arresters [3], [5]-[9]: sealing loss, superficial pollution, varistors degradation, internal humidity, displacement along the active column, and non-uniform voltage distribution.

The purpose of testing different surge arresters samples with several distinct operating conditions was to evaluate the capability of the proposed technique to detect these conditions by analyzing only the total current, i.e., proving that it is possible to perform the MOSA monitoring and the identification of different operating conditions from the total leakage current measurement and analysis, without obtaining the resistive component of the current or employing complex measurement arrangements.

The evaluated MOSA operating conditions are described below.

B. Evaluated MOSA Operating Conditions

The first condition considered in the testing of the MOSA was the good condition. In this case, the tested surge arresters presented characteristics and behaviors similar to the nominal ones. Then, typical failures found in ZnO surge arresters were artificially inserted in the evaluated samples. The faulty conditions are described:

- **Sealing loss:** characterized by the loss of physical isolation between the environment and the interior of the surge arrester, allowing the exchange of gases. The loss of sealing was created artificially in the laboratory by opening communication channels between the environment and the interior of the arrester, allowing the exchange of heat and gas.
- **Internal humidity:** can occur in surge arresters due to failures in the manufacturing process at the moment of the sealing, or by sealing loss caused by the natural aging process of the equipment. To simulate this defect, the arresters were opened and water was aspersed in the varistor column. Then, the arrester was closed.
- **Superficial pollution:** occurs due to the presence of pollution on the surge arrester housing. To simulate this defect, a salt suspension was aspersed on the entire porcelain of the surge arrester.
- **Varistor degradation:** can occur due to natural or precocious varistor aging. To simulate this failure in laboratory, damaged varistors were inserted in the arrester active column. The varistors were damaged by the electrical stress produced by the application of current impulses and overvoltages.
- **Displacement along the active column:** generally occurs due to inadequate transportation or storage of the surge arresters. However, this kind of problem may be caused by the manufacturing process due to assembly errors. In the simulation, displacements in the active column were performed.
- **Non-uniform voltage distribution:** occurs due to failures in the arrester project or superficial pollution on the arresters. In the simulation of this kind failure, several assemblies were used with internal short-circuited varistors, therefore, modifying the electrical field distribution along the arrester.

IV. Feature Extraction Procedure

The next step in the methodology consisted of extracting relevant features of current signal to enable the creation of rules to distinguish the surge arrester operating conditions. The distortion level and the magnitude of the current in MOSA are important indicators of the surge arrester degradation level [1]-[4]. So, it is reasonable to think that the harmonic components of the total current signal constitute a set of features for the effect of monitoring and diagnosing MOSA.

Here, the extraction of the harmonic components of current signal was performed by an adapted version of the parametric identification technique proposed in [10], which consists of automatically determining the parameters of the equation (mathematical model) that represents the behavior of MOSA in a low current region. To determine the best model that self-adapts well to the measured current signals, several tests and adjustments on the model were made. After this, it was found that the model which best represented the measured data was (1) which consists in the sum of the first five odd harmonic components of the signal.

$$s(t) = \sum_{i=1}^{5} A_i \cos\left[(2i-1)\omega t + \theta_i\right] \tag{1}$$

The identification parameter technique is based on the Non Linear Least Squares method associated to the Levenberg-Marquardt optimization algorithm. The technique is used to estimate the parameters (magnitude and phase angles) of (1), so as to minimize the error between the signal reconstructed from the model with identified parameters and the measured signal, i.e., to minimize the following equation (objective function):

$$f(\mathbf{x}) = \frac{1}{2}\sum_{j=1}^{m}\left[r_j(\mathbf{x})\right]^2 = \frac{1}{2}\mathbf{r}(\mathbf{x})^{\mathrm{T}}\mathbf{r}(\mathbf{x}) \tag{2}$$

where the $\mathbf{r}(\mathbf{x})$ function ($\mathbf{r}(\mathbf{x})^{\mathrm{T}}$ is the transpose of $\mathbf{r}(\mathbf{x})$) is called residual and is defined by:

$$\mathbf{r}(\mathbf{x}) = \mathbf{s}_m - \mathbf{s}_c \tag{3}$$

where:

$\mathbf{x}$ n-dimensional parametric vector $\mathbf{x} = (A_i, \theta_i)$ for $i = 1,\ldots,5$;

k is the number of samples in the total current signal;

$\mathbf{s}_m$ is a k-dimensional vector corresponding to measured and digitalized current signal;

$\mathbf{s}_c$ is a k-dimensional vector corresponding to reconstructed signal obtained from application of $\mathbf{x}$ in (1).

To obtain a vector $\mathbf{x}$ that minimizes (2), the updates given by (4) must be performed, until a pre-established stopping criteria (invariance on (2), for example) of the iterative procedure is satisfied.

$$\mathbf{x} = \mathbf{x}_0 + \mathbf{d} \tag{4}$$

where $\mathbf{x}_0$ corresponds to an initial guess of the parameters to be determined (magnitudes and phase angles of harmonic components) and $\mathbf{d}$ (search direction) is the update given to parametric vector $\mathbf{x}$ on each iteration of Levenberg-Marquardt method, with the purpose of minimizing (2).

The search direction, $\mathbf{d}$, is obtained by the resolution of the following system of equations:

$$\mathbf{H}\cdot\mathbf{d} = -\mathbf{g} \tag{5}$$

where $\mathbf{H}$ and $\mathbf{g}$ correspond to the Hessian matrix with the update of the Levenberg-Marquardt method, and to the gradient of the objective function (2), respectively.

The gradient and the Hessian matrix can be obtained in terms of the Jacobian matrix of $\mathbf{r}(\mathbf{x}_0)$ as shown in (6) and (7), respectively. The damping factor μ in (7) is a strategy of the optimization method to guarantee that the Hessian is positive definite and the search direction always conducts to local minimizer of (2). $\mathbf{I}$ is the identity matrix.

$$\mathbf{g} = \mathbf{J}(\mathbf{x})^{\mathrm{T}}\mathbf{r}(\mathbf{x}) \tag{6}$$

$$\mathbf{H} = \mathbf{J}(\mathbf{x})^{\mathrm{T}}\mathbf{J}(\mathbf{x}) + \mu\mathbf{I} \tag{7}$$

where the Jacobian matrix is given by:

$$\mathbf{J}(\mathbf{x}) = \left[\frac{\partial r_i}{\partial x_j}\right]_{\substack{i=1,2,\ldots,k \\ j=1,2,\ldots,n}} \tag{8}$$

V. Feature Extracted Database Building

Since the total current features (harmonic components) have been extracted, it is possible to build a feature database of the all measured signals. This database is utilized in the training and testing of the MOSA operating condition classifier.

The set of model parameters returned by the feature extraction method, $\mathbf{x} = (A_i, \theta_i)$ for $i = 1,\ldots,5$, correspond to the amplitudes and phase angles of the evaluated harmonic components of the signal. After some analysis, it was observed that the phase angles did not provide good correlation of the signal and the MOSA condition, since there is not any phase angle of reference. So, the phase angles are discarded in the construction of the database. Another important pre-processing phase on database building was the normalization of the harmonic amplitudes in relation to the fundamental component. After this, the fundamental component can be omitted from the final database.

With these pre-processing phases, the dimensionality of the problem is reduced to only 4 input variables, the normalized amplitudes of the remaining harmonic components. Finally, it was constructed two feature database. The first one is applied to identify just the MOSA operation condition, i.e., if the surge is defective (label *def*) or not (label *ok*). The second database is composed by labels that identify not only the arrester condition, but the type of failure present in the equipment. In Table I are presented the labels used for each one of the surge arresters evaluated operation conditions.

TABLE I
LABELS FOR MOSA OPERATION CONDITION

Operation condition	Label
Label type 1	
Good	*ok*
Defective	*def*
Label type 2	
Sealing loss	*est*
Internal humidity	*umi*
Superficial pollution	*pol*
Varistor degradation	*deg*
Displacement along the active column	*des*
Non-uniform voltage distribution	*dis*

Therefore, the general format of the databases is as shown in Table II, where the section *Inputs* refers the normalized amplitudes of the parameter vector **x** and the section *Outputs* refers to the MOSA operation condition labels shown in Table I, for each type of label.

TABLE II
GENERAL FORMAT OF EVALUATED DATABASES

Inputs				Outputs
A_2 / A_1	A_3 / A_1	A_4 / A_1	A_5 / A_1	Label

VI. OPERATION CONDITION CLASSIFIER

In this work a operation condition classifier based on a special kind of Neural Networks is used. The is called Self-Organizing Map (SOM) [11]. The SOM network is based on competitive learning and non supervised training algorithm of the type *feed-forward*. In SOM network, the artificial neurons are put on nodes of a neural grid (usually one-dimensional or two-dimensional) with hexagonal, rectangular or triangular topological forms. Each neuron is connected to all network inputs.

The network has a basic topology of two layers: the input layer *I*, responsible for reading the input vector and present to the network the information to be classified; and the output layer *U*, which form a response. The network input corresponds to a vector in the *d*-dimensional space in $\Re^d$, represented by: $x_k = [\xi_1, \ldots, \xi_d]^T$, ($k = 1, \ldots, n$), where n is the number of input vectors. Each neuron j for the output layer holds a code vector **w**, also in $\Re^d$ space, associated to the input vector x_k, $w_j = [w_{j1}, \ldots, w_{jd}]^T$.

The neurons of the SOM network are locally interconnected by a relation of neighborhood, determining the map topology. In a two-dimensional map, the vicinity may be hexagonal or rectangular. The Fig. 3 displays an arrangement with rectangular neighborhood of dimension $X \times Y$. In the same figure, it is observed the winner neuron (green) and its immediate vicinity with six neurons (red). The shape of the arrangement directly influences the adaptation of the SOM network, where the hexagonal model traditionally provides best results than the rectangular ones [11].

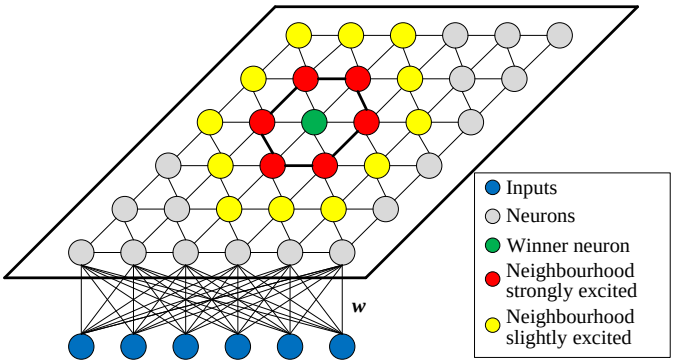

Fig. 3 . Example of bi-dimensional (X × Y) SOM network.

The sequential learning algorithm of the SOM network is composed by three stages: (*i*) competition, (*ii*) cooperation and (*iii*) adaptation. In the competition stage, for each input data presented to network, the neurons compute the activation values and the one with higher value is the winner of the competition or the *Best Match Unit* (BMU). In the second stage (cooperation) is defined the vicinity of the BMU according with an neighborhood function $h(t)$. In the last stage (adaptation), the code vectors (weights) of the winner neuron and of its neighborhood are adjusted. With the adjustment of the code vectors, the response of the winner neuron is better for a subsequent application of the same input vector. So, the input data provide a topological organization of the network neurons.

A. Training Module

The operation condition classifier has training module, as shown in Fig. 1. In this module, the built databases are processed and used on the SOM network training. After this phase the SOM network will be topologically adjusted to recognize new patterns and grouping according their similarities.

B. Classification/Diagnosis Module

On the classification/diagnosis module is implemented the methodology to identify the correlation level between each class (defective or not) of the trained network with the evaluated signal. So, it is possible determine the arrester condition.

Additionally, during the train phase, the classification module can be used to yield a estimative of the classifier hit ratio. This is possible because in the training phase some pairs MOSA conditions and current signal are known in advance. Thus, if the arrester condition estimated by network coincide with the desired condition, the classifier hit in the arrester diagnose. Otherwise, the classification error rate is increased.

VII. RESULTS

There is a set of mechanisms to evaluate the quality of the map obtained after the learning process, such as the vectorial quantization error [11]. The quantization error (E_q) corresponds to the average of the error related to difference between the characteristics vector (x_k) and the code vector

(w_{BMU}), which is the winner code vector in the competitive process to input x_k:

$$E_q = \frac{\sum_{k=1}^{n} \| x_k - w_{BMU} \|}{n}. \quad (9)$$

To evaluate the accuracy of the system, it was used the Correct Classification Rate (*CCR*), which is defined by:

$$CCR = \frac{c}{t} \times 100, \quad (10)$$

where c is the number of data input correctly classified and t is the total number of data input.

The choice by the network size does not follow well defined rules. There are some heuristics rules, but it is consensus among the researchers that it must to test several network configurations before to decide the best parameters for a specific data set [11]. For great data sets, normally, large maps are more adequate. However, there are losses in algorithm training performance. An equilibrium point between the map (grid) size and the accuracy must be found. So, the hit ratio (CCR), the quantization error (Eq), and training time (Tp) of the network were plotted for SOM nets with grids varying of 3x3 until 22x22 (n x n, means n neurons on the two-dimensional space). The parameters of comparison were normalized with relation to the maximum value obtained during the tests for made the analysis independent of the computational system and make easy the results visualization.

In the Figs. 4 and 5 the evolution of comparative parameters in function of the neural grid dimension are plotted. The Fig. 4 corresponds to results of the MOSA condition classifier when it was interested just in diagnosis the surge arrester as defective or not, i.e., when the network was trained and tested with database with labels type 1, as shown in Table I. In Fig. 5 the results of classification system for the database with labels type 2 are shown. In this case, it was evaluated the ability of the classifier in the identify the type of failure on the surge arrester.

As shown in Fig. 4, hit ratios approximately equal to 0.98 (98%) and quantization errors less than 0.2 (20% of the biggest registered value) were obtained for neural grids greater than 15x15. In Fig. 5, similar results were obtained for neural grids greater than 16x16, i.e., it was obtained hit ratios approximately equal to 98% and quantization errors less than 0.2. The necessity of increase the neural grid in second situation (database with labels type 2), it is due the increase in the problem complexity, since the network needs clustering and classifying not only the MOSA condition (defective or not), but the type of failure among those simulated in laboratory. Anyway, the increment in the network is practically irrelevant to retain the same ability of classification. It was concluded that due the uniform performance of the classification system, neural grids with 16x16 neurons yields accurate results on the estimation of the MOSA operation condition and on the identification of type of failure present in surge arrester.

Finally, Fig. 6 shows the final state of a typical 15x15 SOM network after the training phase. As can be seen, the patterns in the database labeled type 1 (*def* or *ok*) were grouped into distinct regions of the map. Therefore, in future tests, to inform new patterns to the neural network, regions marked with labels *def* or *ok* are activated, depending of the characteristics of total leakage current signal of the evaluated surge arrester. So, it is possible to obtain a graphical, intuitive, and accurate result with this kind of classification system, performing the analysis only of the total leakage current of the surge arrester in steady-state operation condition.

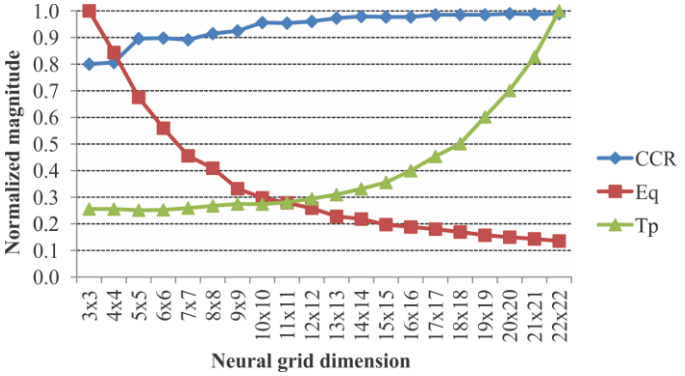

Fig. 4 Evolution of the classifier comparative parameters in the condition identification.

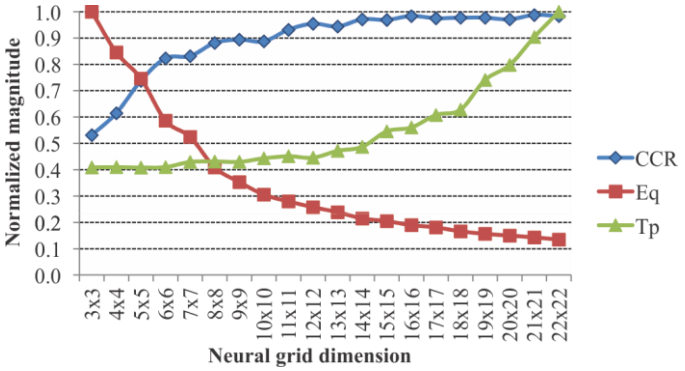

Fig. 5 Evolution of the classifier comparative parameters in the condition classification.

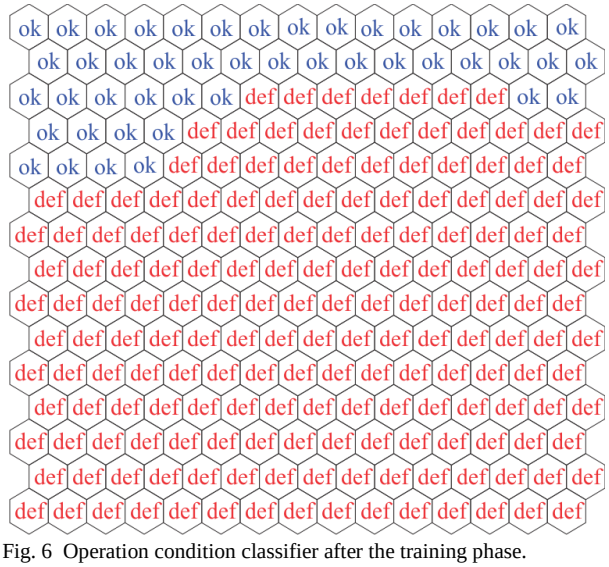

Fig. 6 Operation condition classifier after the training phase.

VIII. Conclusions

In this paper a new surge arrester monitoring and diagnosis technique was presented. The technique is based on analysis of only the total leakage current of the surge arresters when in steady-state operation condition. The techniques existent in the literature, usually require the measurement on site of the surge arrester applied voltage, with the purpose of estimate resistive component of the total leakage current. Measuring high voltage on site consist in a limiting for these techniques, because of the power utilities operational restrictions and inaccuracies on the procedures.

With the proposed technique is not necessary measure or estimate the applied voltage on the surge arrester. It is sufficient to measure the total leakage current, to apply algorithms for feature extraction and classification, for determine the MOSA operation condition.

For extract features of the total current, a methodology able of identify the harmonics components of the current was developed. The extracted features were used in the training and testing process of the surge arrester operation condition classifier. The classifier is based on utilization of a neural network called Self-Organizing Maps (SOM network), which is able to perform the automatic clustering of patterns (current signals) according the patterns level of similarity.

High hit ratios were obtained (greater than 98%) with the proposed technique in the process of classification of the MOSA operation condition (defective or not) and in the identification of the MOSA defect (among those simulated in laboratory). So, it is concluded that is possible to perform the monitoring and diagnosis of ZnO surge arrester, with high accuracy, from the analysis only of the total leakage current.

IX. References

[1] S. Shirakawa, F. Endo, H. Kitajima, S. Kobayashi, K. Kurita, K. Goto, and M. Sakai, "Maintenance of Surge Arrester by a Portable Arrester Leakage Current Detector," *IEEE Trans. Power Del.*, vol. 3, no. 3, pp. 998–1003, Jul. 1988.

[2] J. Lundquist, L. Stenstrom, A. Schei, and B. Hansen, "New method for measurement of the resistive leakage currents of metal-oxide surge arresters in service," *IEEE Trans. Power Del.*, vol. 5, no. 4, pp. 1811–1822, Oct. 1990.

[3] C. Heinrich and V. Hinrichsen, "Diagnostics and Monitoring of Metal-Oxide Surge Arresters in High-Voltage Networks-Comparison of Existing and Newly Developed Procedures," *IEEE Trans. Power Del.*,vol. 16, no. 1, pp. 138–143, Jan. 2001.

[4] *Surge Arresters - Selection and Application Recommendations*, IEC Standard 60099-5, 2000.

[5] G. R. S. Lira, "Monitoramento de Para-raios de Óxido de Zinco com Base na Medição da Corrente de Fuga Total," D.Sc. Thesis, Departamento de Engenharia Elétrica, Universidade Federal de Campina Grande, 2012.

[6] E. T. Wanderley Neto, E. G. da Costa, and M. J. A. Maia, "Artificial Neural Networks Used for ZnO Arresters Diagnosis," *IEEE Trans. Power Del.*, vol. 24, no. 3, pp. 1390–1395, Jul. 2009.

[7] G. R. S. Lira, E. G. Costa, and C. W. D. Almeida, "Self-organizing maps applied to monitoring and diagnosis of ZnO surge arresters," in *Proc. IEEE/PES Transmission and Distribution Conf. and Expo.: Latin America*, Nov. 2010, pp. 659–664.

[8] K. L. Chrzan, "Influence of Moisture and Partial Discharges on the Degradation of High-Voltage Surge Arresters," *Euro. Trans. Electr. Power*, vol. 14, no. 3, pp. 175–184, May 2004.

[9] K. Feser, W. Khler, D. Qiu, and K. Chrzan, "Behaviour of Zinc Oxide Surge Arresters Under Pollution," IEEE Trans. Power Del., vol. 6, no. 2, pp. 688–695, Apr. 1991.

[10] G. R. S. Lira, D. F. Jr., and E. G. Costa, "Parameter identification technique for a dynamic metal-oxide surge arrester model," in *Proc. Int. Conf. on Power Systems Transients*, Jun. 2009.

[11] T. Kohonen, *Self-Organizing Maps*. Springer; 3rd ed. edition, 2000.